Critical study of photodetachment of H^- at energies up to the n=4 threshold

Jian-Zhi Tang,[1] Yoshihiro Wakabayashi,[2] Michio Matsuzawa,[2]
Shinichi Watanabe,[2] and Isao Shimamura[1]

[1] *The Institute of Physical and Chemical Research (RIKEN), Wako, Saitama 351-01, Japan*
[2] *Department of Applied Physics and Chemistry, The University of Electro-Communications, Chofu-shi, Tokyo 182, Japan*

(Received 2 July 1993)

We apply the close-coupling method in terms of the hyperspherical coordinates to the two-electron system H^-. A two-dimensional matching procedure is used to connect the close-coupling wave function to an independent-electron wave function in the asymptotic region. The latter is described as the wave function of a detached electron moving in a dipole potential field of the neutral hydrogen atom. The total photodetachment cross sections and the partial cross sections for the production of the H atoms in different states n are calculated up to the n=4 hydrogenic threshold. The results obtained in the length and acceleration forms agree within about three significant figures. The magnitude and shape of the $^1P^o$ shape resonance just above the n=2 threshold are found to depend sensitively on the initial-state wave function. This appears to be one of the reasons for a disparity among the cross sections in the literature. The present result improves greatly on the existing computational results. The relative magnitudes of the partial cross sections for the production of H (n=1,2,3) atoms below the n=4 threshold are substantially different from the only previous results of the eigenchannel R-matrix calculations [H. R. Sadeghpour, C. H. Greene, and M. Cavagnero, Phys. Rev. A **45**, 1587 (1992)]. The present results on both partial and total cross sections are in excellent agreement with experiments.

PACS number(s): 32.80.Fb, 31.20.Di, 31.50.+w

I. INTRODUCTION

Photodetachment and photoionization spectra of two-electron systems H^-, He, and He-like positive ions are rich in structures. These structures are attributed to doubly excited states and are particularly useful in understanding the strong electron-electron correlations in the two-electron systems.

The final continuum state of photoionization of the He atom or He-like positive ions is influenced by the attractive Coulomb tail of the interaction potential at large distances r between the ejected electron and the residual ion core. On the other hand, the final state of photodetachment of the H^- ion, leaving a hydrogen atom in an excited state n, is influenced by the asymptotic potential of the form $\sim r^{-2}$. This asymptotic dipolelike potential stems from the centrifugal potential and the permanent dipole moment of the H(n) atom [1,2]. It is usually overshadowed by the Coulomb potential in photoionization of He and He-like positive ions.

Doubly excited states of H^- of $^1P^o$ symmetry, including the shape resonance just above the H(n=2) threshold, have been known theoretically for some time [3,4]. These resonances have been observed first in electron scattering by the hydrogen atom [5,6] and later in photodetachment of H^- in the presence and absence of the electric field [7–11]. The high-resolution power of the photodetachment experiments allows even high-lying doubly excited states to be resolved.

Accurate *ab initio* calculations of the cross sections for photodetachment of H^- are few [12–15], especially at photon energies near the n=3 threshold and above; discrepancy is found among these calculations, even for the broad shape resonance just above the n=2 threshold. Recently, the eigenchannel R-matrix method has been applied in a broader energy region ranging up to the n=4 threshold [15]. The partial cross section calculated for the production of the H(n=2) atoms is larger than that for the production of the H(n=1) atoms at energies below the n=4 threshold. This is difficult to understand in nonresonant photodetachment, which is induced by a one-electron dipole operator. The H(n=1) production is a one-electron excitation process, while the H(n=2) production is a two-electron excitation process with one electron detached and the other excited; the latter process occurs only through the electron-electron correlation or configuration mixing. Thus the results from the R-matrix calculations [15] should be confirmed and physically interpreted.

We have recently proposed an accurate and powerful computational method, the hyperspherical close-coupling (HSCC) method, for two-electron atoms [16]. This method takes advantage of the hyperspherical coordinates [17], i.e., a pair of collective variables R and α, which replace the independent-electron radial coordinates r_1 and r_2. The hyperradius $R = \sqrt{r_1^2 + r_2^2}$ measures the "size" of the electron pair and the hyperangle $\alpha = \arctan(r_2/r_1)$ describes the degree of radial electron-electron correlation. The accuracy and efficiency of the method have been demonstrated on various physical quantities of He [16, 18–20].

In this paper, we apply the HSCC method to study the

role played by doubly excited states in the photodetachment of H^- at photon energies up to the n=4 threshold. A two-dimensional matching procedure [16] is used to connect the HSCC wave function to the wave function of the detached electron, which is described as moving in the asymptotic potential of the form $\sim r^{-2}$. Excellent agreement with experimental cross sections is found. Initial-state wave functions of varying degrees of accuracy are used, and the photodetachment cross sections calculated are found to be sensitive to the choice of the wave functions.

Section II gives a brief description of the HSCC method and the asymptotic solutions. Calculated results are discussed and compared in Sec. III with experimental as well as other theoretical results. Finally, Sec. IV summarizes this work. Atomic units are used throughout this paper unless otherwise specified.

II. HYPERSPHERICAL CLOSE-COUPLING METHOD

The hyperspherical-coordinate method [17] has played a prominent role in describing the strong electron-electron correlations in two-electron systems, such as He and H^-. The approximate separability of the motion in the hyperradius R from the motion in the hyperangle α provides a simple and transparent physical picture for understanding the properties of doubly excited states. For accurate computations, however, we need to go beyond this adiabatic approximation. We have developed the close-coupling method that couples the adiabatic states in terms of the hyperspherical coordinates. We refer to this method as the hyperspherical close-coupling method [16, 18]. Here we briefly review the computational procedure involving the HSCC method.

We divide the whole configuration space into two, namely, the inner region specified by $R \le R_{\rm HS}$ with a certain constant $R_{\rm HS}$, and the outer region $R \ge R_{\rm HS}$. We define the inner-region adiabatic Hamiltonian

$$H_{\rm ad} = \Lambda^2 - 2RC - \frac{1}{4} \quad (R \le R_{\rm HS}) \tag{1}$$

with the grand-angular-momentum operator

$$\Lambda^2 = -\frac{\partial^2}{\partial\alpha^2} + \frac{\mathbf{l}_1^2}{\cos^2\alpha} + \frac{\mathbf{l}_2^2}{\sin^2\alpha} \tag{2}$$

and the total Coulomb potential

$$C(\alpha,\theta_{12}) = \frac{1}{\cos\alpha} + \frac{1}{\sin\alpha} - \frac{1}{\sqrt{1-\sin 2\alpha\cos\theta_{12}}} \tag{3}$$

of the three-body system H^-. The position vectors of the two electrons are $\mathbf{r}_1$ and $\mathbf{r}_2$, the corresponding single-electron angular-momentum operators being $\mathbf{l}_1$ and $\mathbf{l}_2$, and θ_{12} is the angle between $\mathbf{r}_1$ and $\mathbf{r}_2$.

We define an orthogonal set of diabatic basis functions at each fixed value of R and for each pair of angular momenta (l_1, l_2) by [16]

$$\phi_\nu^{LM}(\alpha,\hat{\mathbf{r}}_1,\hat{\mathbf{r}}_2;R) = g^\mu_{l_1 l_2}(\alpha;R)\mathcal{Y}^{LM}_{l_1 l_2}(\hat{\mathbf{r}}_1,\hat{\mathbf{r}}_2), \tag{4}$$

where ν refers collectively to the set (μ, l_1, l_2). The angular function $\mathcal{Y}^{LM}_{l_1 l_2}$ is an eigenfunction of $(\mathbf{l}_1+\mathbf{l}_2)^2$ and $(\mathbf{l}_1+\mathbf{l}_2)_z$ with eigenvalues $L(L+1)$ and M and is formed by coupling spherical harmonics $Y_{l_1 m_1}(\hat{\mathbf{r}}_1)$ and $Y_{l_2 m_2}(\hat{\mathbf{r}}_2)$. The function $g^\mu_{l_1 l_2}$ is an eigenfunction of $(\mathcal{Y}^{LM}_{l_1 l_2}|H_{\rm ad}|\mathcal{Y}^{LM}_{l_1 l_2})$. This eigenfunction has a fixed number of nodes in α over the whole region of R and approaches a hyperspherical harmonic as $R \to 0$ and a hydrogenic wave function as $R \to \infty$. An accurate and efficient numerical scheme for setting up these basis functions has been developed [16]. This scheme dictates the precision of the whole method.

Let $\Psi^{(\rm in)}_\beta(R,\alpha,\hat{\mathbf{r}}_1,\hat{\mathbf{r}}_2)$ be the (L,M) component of the total wave function of the two-electron system in the inner region, the subscript specifying the βth independent solution and the quantum numbers L and M being suppressed. This total wave function is expanded in terms of the diabatic basis functions (4) as

$$\Psi^{(\rm in)}_\beta = (R^{5/2}\cos\alpha\sin\alpha)^{-1}\sum_\nu F_{\nu\beta}(R)\phi_\nu(\alpha,\hat{\mathbf{r}}_1,\hat{\mathbf{r}}_2;R)$$
$$(R \le R_{\rm HS}), \tag{5}$$

and the Schrödinger equation is cast into close-coupling equations for $F_{\nu\beta}(R)$. This expansion has been found to converge monotonically and rapidly for He [16, 18–20]. The well-established accurate methods for solving close-coupling equations may be used without serious practical difficulties, just as in the previous applications to photoionization of He. The solutions are propagated out to $R = R_{\rm HS}$.

In the asymptotic region where one electron lies far from the hydrogen atom, the conventional independent-electron picture is more appropriate than the hyperspherical-coordinate description. Therefore, the wave function $\Psi^{(\rm out)}_\beta(R,\alpha,\hat{\mathbf{r}}_1,\hat{\mathbf{r}}_2)$ in the outer region is expanded in terms of the hydrogenic states with radial wave functions $u_{nl_1}(r_1)$. Then the interaction potential matrix for electron 2 takes an asymptotic form [1, 2]

$$\begin{aligned} V_{ii'}(r_2) &= \frac{D_{ii'}}{2r_2^2} + \mathcal{O}(r_2^{-3}) \\ &= r_2^{-2} < u_{nl_1}\mathcal{Y}^{LM}_{l_1 l_2}|\tfrac{1}{2}\mathbf{l}_2^2 + \mathbf{r}_1\cdot\hat{\mathbf{r}}_2|u_{n'l_1'}\mathcal{Y}^{LM}_{l_1' l_2'} > \delta_{nn'} \\ &\quad + \mathcal{O}(r_2^{-3}) \quad (r_2 \to \infty). \end{aligned} \tag{6}$$

The matrix element $D_{ii'}$ consists of the centrifugal potential diagonal in l_2 and the dipole transition matrix, which represents the exchange of angular momentum between electron 2 and the hydrogen atom. Only the asymptotic potential (6) is retained in the whole outer region in the present work.

Diagonalize the matrix $D_{ii'}$ and obtain the eigenvalues a_j and the corresponding unitarily transformed channel functions $\varphi_j(\mathbf{r}_1,\hat{\mathbf{r}}_2)$. This leads to a set of uncoupled radial equations

$$\left(-\frac{d^2}{dr_2^2} + \frac{a_j}{r_2^2} - k_n^2\right)Z_j(r_2) = 0, \tag{7}$$

where $\frac{1}{2}k_n^2 = \epsilon_n$ is the channel energy, or the total energy E plus the binding energy $1/2n^2$ of the hydrogen atom.

If we write $a_j = \tilde{l}_j(\tilde{l}_j+1)$, $\tilde{l}_j$ may be regarded as a

modified angular momentum of a transformed channel j. The modified angular momentum takes a real number if $a_j \geq -\frac{1}{4}$. On the other hand, $\tilde{l}_j + \frac{1}{2}$ is pure imaginary if $a_j < -\frac{1}{4}$. In this latter case, the potential in the uncoupled equation (7) supports an infinite series of bound states at energies $\epsilon_{n,n'}$, labeled by n' [21]. This series turns into an infinite series of resonances when coupled with open channels [2].

The solutions of each uncoupled equation are of the Bessel class of order $\pm(\tilde{l}_j+\frac{1}{2})$ and are well known [1,2,22]. For open channels, for which $k_n^2 > 0$, we may find two linearly independent solutions $s_j(k_n r_2)$ and $c_j(k_n r_2)$ that are energy normalized. For closed channels, for which $k_n^2 < 0$, we may find a solution $f_j(r_2)$ that decays exponentially with r_2. Then we may express the (L,M) component of the total wave function in the outer region as

$$\Psi_\beta^{(\mathrm{out})} = r_2^{-1} \sum_{j,\mathrm{open}} \varphi_j(\mathbf{r}_1, \hat{\mathbf{r}}_2)[s_j(k_n r_2) I_{j\beta} - c_j(k_n r_2) J_{j\beta}] + r_2^{-1} \sum_{j,\mathrm{closed}} \varphi_j(\mathbf{r}_1, \hat{\mathbf{r}}_2) f_j(r_2) C_{j\beta} \quad (R \geq R_{\mathrm{HS}}), \tag{8}$$

the first summation being taken over only open channels and the second over only closed channels.

The two-dimensional matching [16] of the wave functions $\Psi_\beta^{(\mathrm{in})}$ and $\Psi_\beta^{(\mathrm{out})}$ on the surface $R = R_{\mathrm{HS}}$ determines the coefficients $I_{j\beta}$, $J_{j\beta}$, and $C_{j\beta}$. The reaction matrix K follows from the coefficients $I_{j\beta}$ and $J_{j\beta}$ according to the standard procedure. A wave function that satisfies the asymptotic boundary condition for the final state of photodetachment is expressible as a linear combination of independent solutions $\Psi_\beta^{(\mathrm{out})}$ in terms of the K matrix.

When all channels are closed, i.e., when $E < -\frac{1}{2}$, the outer-region wave function satisfies the condition (8) (without the first sum) only at particular energies. These energies are bound-state energies. A convenient method of finding bound states is to write each channel wave function as a linear combination of the exponentially decaying and growing solutions of Eq. (7) and to define a matrix similar to the K matrix for open channels. Calculate the determinant of this matrix as a function of the energy E and find zeros. The condition (8) is satisfied at these zeros. The initial wave function for photodetachment of H^- may be calculated in this way.

Reference [18] details the numerical procedure for the matrix element of the dipole transition operator between the initial and final wave functions. In fact, the main ingredients are produced as the hyperspherical close-coupling wave functions are propagated out and are finally assembled into the dipole matrix element by use of the K matrix [20].

III. RESULTS AND DISCUSSION

A. Wave functions and classification scheme

The quality of the wave function for the initial state of photodetachment of H^-, i.e., the ground ^1S state, is expected to be a decisive factor for the accuracy of the dipole matrix element. This is partly because the overlap integral between the initial and final states is small and partly because the wave function for this weakly bound initial state decays slowly with R as $\sim\exp(-\kappa R)$. The rate of this decay depends sensitively on the ground-state energy E_0 through the relation

$$\frac{1}{2}\kappa^2 = -\frac{1}{2} - E_0, \tag{9}$$

the right-hand side being the binding energy. We may refer to κ^{-1}, having the dimension of length, as the size parameter.

For the purpose of studying the sensitivity of the photodetachment cross sections to the initial-state wave function, we calculate E_0 by retaining different numbers N_{ch} of diabatic channels in the wave function (5). The close-coupling equations are integrated up to $R = 36$. This value is found to be large enough for the convergence of not only the calculated energies but also the dipole matrix elements in the length form, which weigh a region of larger R than those in the velocity or acceleration form.

Table I lists the calculated energies together with the corresponding size parameters κ^{-1} and compares them with previous accurate calculations by Pekeris [23] and with an experimental value [24]. Channels that asymptotically approach the configurations $1s\epsilon s$, $2p\epsilon p$, $2s\epsilon s$, etc., are numbered 1, 2, 3, etc. A rapid convergence in

TABLE I. The energy E_0 of the ground state of H^- and the size parameter κ^{-1} of Eq. (9) calculated with different numbers N_{ch} of diabatic channels in Eq. (5).

N_{ch}	E_0 (a.u.)	κ^{-1} (a.u.)
2	−0.51543	5.692
3	−0.52723	4.285
6	−0.52755	4.260
10	−0.52765	4.252
21	−0.52772	4.247
28	−0.52773	4.246
Accurate theoretical value (Ref. [23])	−0.52775	4.245
Experimental value (Ref. [24])	−0.52773 ±0.00001	4.246

E_0 with N_{ch} is clearly seen. Even the energy -0.5272 calculated with only the first three channels coupled is already close to the converged value of -0.5277. This implies a crucial importance of the coupling in the internal region between the n=1 and n=2 channels compared with that between the n=1 and $n > 2$ channels. This feature was also found for the ground state of helium [18]. The three-channel result for H^- is more accurate than the value -0.5240 calculated in Ref. [15], which uses the eigenchannel R-matrix method with 158 two-electron configurations within the R-matrix box defined by $\max(r_1, r_2) \leq 25$. In the present work, the 21-channel wave function has been adopted as the initial state for the photodetachment calculations, except when less elaborate wave functions are tried just for comparison.

For the final states of photodetachment, i.e., $^1P^o$ continuum states, 36 close-coupling channels are retained in Eq. (5). In other words, all channels that approach asymptotically the H($n \leq 6$) states are retained. The two-dimensional matching procedure is applied at $R = R_{HS} = 200$. The cross sections calculated in the length form agree with those calculated in the acceleration form within about three significant figures.

We use a set of quantum numbers $n(K,T)^A_{n'}$ to classify resonances in the final state of photodetachment. The quantum numbers K and T pertain to the angular correlation [25], while A pertains to the radial correlation [26]. The principal quantum number n of the inner electron defines a series of resonances that converges to the H(n) threshold and in which the radial quantum number n' of the outer electron takes on different values [27].

There exist three channels of the form (7) that describe dissociation of the H^- system of symmetry $^1P^o$ into an electron and H(n=2). For these channels, $a_j = -3.7082$, 2.0000, and 9.7082, and hence the modified angular momentum $\tilde{l}_j = -0.5000 + 1.8596i$, 1.0000, and 2.6557. The first channel has an effective potential that is attractive enough for making $\tilde{l}_j + \frac{1}{2}$ pure imaginary and for supporting an infinite number of bound states [2, 21]. These bound states turn into a series of resonance states of type $2(1,0)^-_{n'}$ with radial correlation index $A = -$ converging to the n=2 threshold, when coupled with the open H(n=1) channel. The second channel is a conventional p-wave channel itself, which remains uncoupled with the other conventional channels in the asymptotic region. This is because the 3×3 D matrix in Eq. (6) is block diagonal and consists of 2×2 and 1×1 submatrices; the latter submatrix corresponds to the second channel with $\tilde{l}_2 = 1$. Just as attractive spherical potentials often support p-wave shape resonances [21], the second channel supports a well-known $2(0,1)^+$ shape resonance due to the short-range attractive effective potential and the centrifugal barrier. The third channel is too strongly repulsive and supports no resonances.

The positions $\epsilon_{n,n'}$, with respect to the n=2 threshold, and the widths $\Gamma_{n,n'}$ of the infinite series of resonances converging to this threshold satisfy a relation [2]

$$\frac{\epsilon_{n,n'+1}}{\epsilon_{n,n'}} \simeq \frac{\Gamma_{n,n'+1}}{\Gamma_{n,n'}} \simeq \exp\left\{\frac{2\pi\lambda}{\tilde{l}_j + \frac{1}{2}}\right\} \tag{10}$$

in the nonrelativistic approximation. Only several in this series remain as resonances, if account is taken of the splitting of the hydrogenic sublevels due to the relativistic and quantum-electrodynamic corrections.

Equation (10) applies also to infinite series of resonances of any symmetry that are known to converge to each hydrogenic threshold. Reference [28] tabulates examples of the factor on the right-hand side of Eq. (10) for n=2, 3, and 4 and of a crude estimate of the number of resonances in the presence of the sublevel splitting.

B. Total cross sections

The calculated total cross sections for photodetachment are shown in Fig. 1 and are compared in Fig. 2 with experimental results below the n=3 threshold [10, 11]. In Fig. 2, the calculated results are convoluted with the experimental resolution of 7 meV, and the experimental relative cross sections are normalized for achieving an overall good fit to the theory. The present results are in general and excellent agreement with experiments except at the $2(1,0)^-_3$ resonance on the left of the main peak in Fig. 2(a). Only two of the $2(1,0)^-_{n'}$ resonances are seen in Fig. 1(a). The $2(1,0)^-_4$ resonance is too narrow and too near the broad shape resonance to be visible in the experimental spectra.

The broad $2(0,1)^+$ shape resonance lying 19 meV above the n=2 threshold has been studied by various theoretical methods, namely, the 1s-2s-2p close-coupling method [12], the J-matrix method using square-integrable basis functions [13], the adiabatic hyperspherical-coordinate approach [14], and the eigenchannel R-matrix method [15]. Surprisingly, however, no

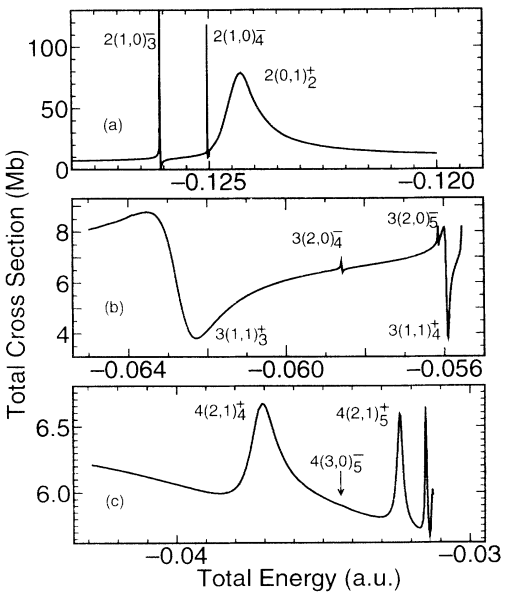

FIG. 1. The total cross section calculated for photodetachment of H^- (a) near the n=2 threshold, (b) below the n=3 threshold, and (c) below the n=4 threshold. See text for the assignment of the resonances $n(K,T)^A_{n'}$. The resonance $4(3,0)^-_5$ occurs at the position of the arrow in (c), but is invisible in the figure.

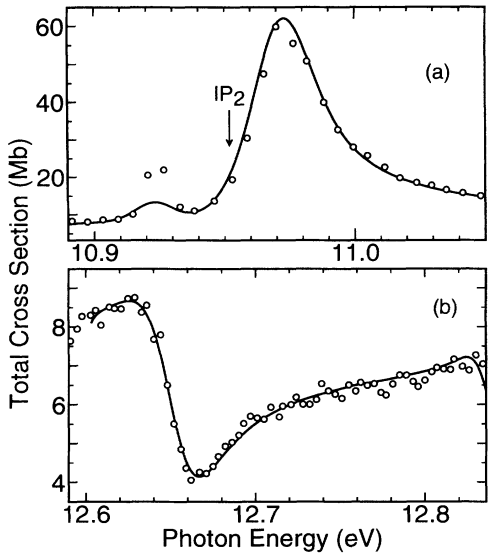

FIG. 2. Comparison of the calculated total photodetachment cross section with experiments (a) near the n=2 threshold and (b) below the n=3 threshold. Solid lines: present calculations convoluted with an experimental resolution of 7 meV. Circles: experimental results of (a) Ref. [11] and (b) Ref. [10] normalized to the calculated cross sections. IP_2: the threshold of the n=2 channel.

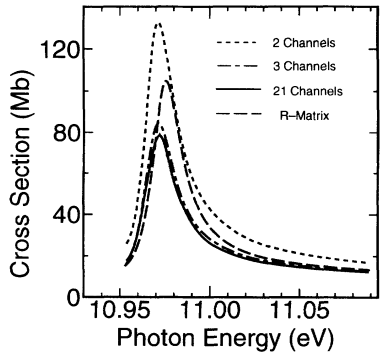

FIG. 3. The profile of the $^1P^o$ shape resonance in the total photodetachment cross section just above the n=2 threshold. The effect of the quality of the initial-state wave function is studied by changing the number of channels in Eq. (5). Comparison is also made with the results of the eigenchannel R-matrix calculations of Ref. [15]. See also Table II.

two previous theories have predicted all of the exact position, width, and the peak cross section in good agreement with each other [11]. The first two methods use continuum wave functions that are less accurate than those used in the present work. The effects of the long-range potential of the form $\sim r^{-2}$ are inadequately taken into account in the J-matrix method [13]. On the other hand, the R-matrix calculations of Ref. [15] use elaborate continuum wave functions. Nevertheless, the present results disagree with the R-matrix results. This disagreement appears to be rooted largely in the quality of the wave function of the initial state, especially the range of the wave function, or the size parameter κ^{-1} of Eq. (9). In support of this view, Fig. 3 compares the cross sections in the shape-resonance region calculated with initial-state wave functions containing 2, 3, and 21 channels; Fig. 3 also includes the results of the eigenchannel R-matrix calculations [15]. As the energy E_0 of the initial state is improved, the profile of the $2(0,1)^+$ shape resonance becomes smaller and narrower. An even clearer indication of the sensitivity of the cross section to the size parameter κ^{-1} is found in Table II, where the results of the J-matrix calculations are also included. We believe that the results from the 21-channel calculations are the most accurate among the values in Fig. 3 and in Table II. We note in passing that this shape resonance was measured for electron scattering by hydrogen atoms and is located at -0.1245 ± 0.0001 with a width of 0.0008 ± 0.0001 [29].

Figure 1(b) of the spectrum below the n=3 threshold and Fig. 1(c) of that below the n=4 threshold illustrate the propensity rule of Ref. [30]. This rule states that the lowest channel with A = + influences the photodetachment spectrum of H^- most strongly among the $2n-1$ channels in each n manifold.

Reference [28] reports the results of R-matrix calculations of 15-state close-coupling equations for electron-hydrogen collisions, i.e., including all the channels associated with the hydrogenic states up to n=5; 48 continuum orbitals have been used for each channel angular momentum within an R-matrix box of size 83.0. These calculations predict not only a series of broad resonances $4(2,1)^+_{n'}$ but also a series of narrow resonances $4(3,0)^-_{n'}$, the lowest of which lies at $E_r = -0.034\,289$ and has a

TABLE II. The peak height σ_{max} (in Mb), the position E_r, and the width Γ of the $2(0,1)^+$ shape resonance lying just above the n=2 threshold. Results of different theoretical methods using ground-state wave functions of different quality are compared. N_{ch} is the number of diabatic channels in Eq. (5). E_0 is the ground-state energy. κ^{-1} is the size parameter of Eq. (9). $6.85[-4] = 6.85 \times 10^{-4}$.

Method	E_0 (a.u.)	κ^{-1} (a.u.)	σ_{max} (Mb)	E_r (a.u.)	Γ (a.u.)
R matrix (Ref. [15])	−0.52403	4.562	104.7	−0.12424	6.85[−4]
J matrix (Ref. [13])	−0.52738	4.273	95	−0.12434	5.5[−4]
Present (N_{ch}= 2)	−0.51543	5.692	132.6	−0.12429	8.09[−4]
Present (N_{ch}= 3)	−0.52723	4.285	84.4	−0.12430	7.70[−4]
Present (N_{ch}=21)	−0.52772	4.247	78.6	−0.12432	6.21[−4]

TABLE III. Resonance energies E_r and widths Γ (in a.u.) of H^- of $^1P^o$ symmetry. $2.40[-6] = 2.40 \times 10^{-6}$.

Classification	Present		Complex coordinate		R matrix		Algebraic close coupling[e]	
	$-E_r$	Γ	$-E_r$	Γ	$-E_r$	Γ	$-E_r$	Γ
$2(1,0)_3^-$	0.12606	2.40[−6]	0.12605[a]	3.8[−5][a]	0.12601[c]	1.06[−6][c]	0.12601	1.37[−6]
					0.12604[d]			
$2(1,0)_4^-$	0.12503						0.12600	1.15[−6]
$2(0,1)_2^+$	0.12432	6.21[−4]	0.12435[a]	5.2[−4][a]	0.12424[c]	6.85[−4][c]	0.12440	7.35[−4]
					0.12433[d]	1.16[−3][d]		
$3(1,1)_3^+$	0.06272	1.20[−3]	0.06272[b]	1.19[−3][b]	0.06270[c]	1.23[−3][c]	0.06272	1.19[−3]
					0.06271[d]	1.26[−3][d]		
$3(1,1)_4^+$	0.05591	5.70[−5]	0.05591[b]	7.0[−5][b]	0.05583[c]	4.26[−5][c]	0.05590	6.85[−5]
					0.05590[d]	6.65[−5][d]		
$3(2,0)_4^-$	0.05859	9.59[−6]	0.05857[b]	8.99[−6][b]	0.05887[c]	1.48[−5][c]	0.05857	8.95[−6]
					0.05857[d]	9.00[−6][d]		
$3(2,0)_5^-$	0.05614		0.05612[b]	2.1[−6][b]	0.05615[d]		0.05612	2.18[−6]
$4(2,1)_4^+$	0.03717	1.03[−3]	0.03718[b]	1.03[−3][b]	0.03718[c]	1.04[−3][c]	0.03717	1.01[−3]
					0.03713[d]	1.25[−3][d]		
$4(2,1)_5^+$	0.03228	1.50[−4]	0.03235[b]	2.44[−4][b]	0.03232[d]	2.25[−4][d]		
$4(3,0)_5^-$	0.03432	1.76[−5]	0.03429[b]	1.83[−5][b]	0.03439[c]	2.67[−5][c]		
					0.03429[d]	1.80[−5][d]		

[a]Reference [32].
[b]Reference [31].
[c]Reference [15].
[d]Reference [28].
[e]Reference [33].

width of $\Gamma = 1.8\times10^{-5}$. This resonance should lie between the $4(2,1)_4^+$ and $4(2,1)_5^+$ resonances in Fig. 1(c). In the eigenchannel R-matrix calculations of photodetachment [15], this resonance is found at $E_r = -0.034\,388$ with a width of $\Gamma = 2.67\times10^{-5}$, and is visible in the length-form results but not in the velocity-form results. The latter form is supposed to lead to relatively more reliable cross sections [15]. In the present calculations, this resonance occurs at $E_r = -0.034\,315$ with a width of $\Gamma = 1.76\times10^{-5}$ in the eigenphase sum in the final-channel wave function. However, this introduces no appreciable structure into the spectrum in Fig. 1(c) in either the length or the acceleration form, unless the figure is enlarged by a few orders of magnitude. In his complex-coordinate calculations of resonance states of H^-, Ho [31] also found this resonance at $E_r = -0.034\,294$ with a width of $\Gamma = 1.83\times10^{-5}$.

The positions and widths of the resonances calculated from the eigenphase sum in this paper are listed in Table III and are compared with the results of other accurate calculations [15, 28, 31–33]. The extensive complex-coordinate calculations of Ref. [31] are seen to be generally in good agreement with our accurate results.

C. Partial cross sections

Figure 4 shows the partial cross sections for the production of the hydrogen atoms in different states n. We see that the H(n=2) partial cross section dominates over the H(n=1) partial cross section in some energy regions of resonances, while the latter is larger in the regions of nonresonant photodetachment. This is reasonable since the photodetachment process off resonance is basically a one-electron process, as is the production of H(n=1). The present results on nonresonant photodetachment below the n=4 threshold [Fig. 4(c)] are seen to be of no exception. This contradicts the results of the eigenchannel R-

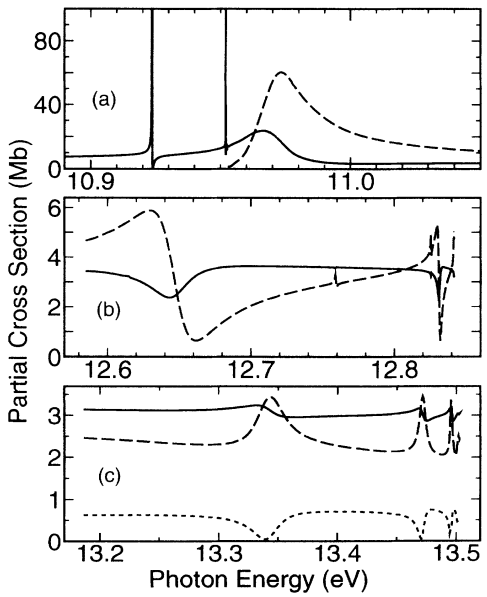

FIG. 4. Calculated partial cross sections for the production of H(n) (a) near the n=2 threshold, (b) below the n=3 threshold, and (c) below the n=4 threshold. Solid line: H(n=1). Dashed line: H(n=2). Dotted line: H(n=3).

matrix calculations of Ref. [15], in which the H(n=2) partial cross section is found to be larger than the H(n=1) partial cross section below the n=4 threshold.

We show in Fig. 5 how the partial cross sections below the n=4 threshold vary with different choices of the initial-state wave function. The H(n=1) partial cross section off resonance dominates over the H(n=2) partial cross section irrespective of the number of channels included in the initial-state calculation. We believe that the present results below the n=4 threshold are more reliable than those of Ref. [15], partly because of the physical considerations in the preceding paragraph and partly because of the agreement between the length- and acceleration-form results of the present work to within about three significant figures; the agreement between the length- and velocity-form results is reported to be within as much as 20% in Ref. [15].

Doubly excited states are often expected to lead predominantly to autodetachment into the nearest available decay channel [30]. However, this expectation should not be confused with that on the actual relative magnitudes of partial photodetachment cross sections. These relative magnitudes depend on the relative probabilities of the formation of doubly excited states and of direct electron detachment [15]. Indeed, Fig. 4(c), for example, shows that the partial cross sections increase with decreasing n in nearly the whole energy region just below the n=4 threshold.

Figure 6 compares the calculated H(n=2) partial cross section with experimental results [10,11] (a) in the energy region of the shape resonance just above the n=2 threshold and (b) in the region just below the n=3 threshold. The agreement is as excellent as for the total cross section in the same region of energy.

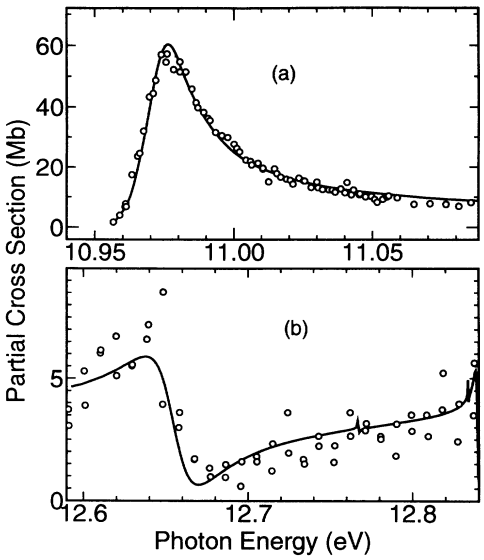

FIG. 6. Comparison of the partial cross section for the production of H(n=2) with experiments (a) near the n=2 threshold and (b) below the n=3 threshold. Solid lines: present calculations without convolution. Circles: experimental results of (a) Ref. [11] and (b) Ref. [10] normalized to fit best to the calculated results.

IV. SUMMARY

We have studied the photodetachment spectrum of H^- up to the n=4 threshold by combining the hyperspherical close-coupling method [16] with an analytic description of the detached electron in the dipole field of the hydrogen atom. The cross sections calculated in the length and acceleration forms agree within three digits in the whole energy range. Both total and partial relative experimental cross sections are excellently reproduced. The partial cross section for the production of the H(n=1) atoms is larger than the H(n=2) partial cross section except in some resonance regions. This remains to be true even in the energy region below the n=4 threshold, which contradicts the results of previous eigenchannel R-matrix calculations [15].

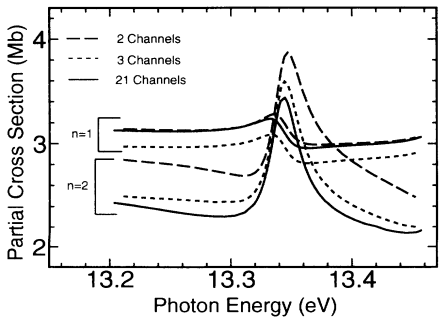

FIG. 5. Partial cross sections for the production of H(n=1) and H(n=2) below the n=4 threshold calculated by changing the quality of the initial-state wave function. The number of channels refers to the terms in Eq. (5).

The electron-electron correlations in the initial state play a significant role in determining accurate total photodetachment cross sections through the precise value of the small electron affinity, which determines the size of the H^- ion. The profile of the shape resonance just above the n=2 threshold, for example, becomes higher and broader when the electron affinity is underestimated.

At present, experimental data are available only on relative values of the cross sections. Furthermore, the experimental errors in the partial cross sections just below the n=3 and the n=4 thresholds are large [10]. Improvements on the experiments are highly desirable for quantitative comparisons with different theories.

Note added. A related paper has been published after the submission of the original manuscript of this paper. Cortés and Martín [34] applied a recently proposed L^2 method to photodetachment of H^- up to the n=3 threshold. The resonance parameters calculated by them agree well with the present results.

ACKNOWLEDGMENTS

One of us (J.Z.T.) was supported by the Special Researchers' Basic Science Program of Science and Tech-

nology Agency, Japan. We would like to thank Professor Bryant and Dr. Halka for providing us with their experimental data and Dr. Sadeghpour for providing us with calculated results. The work reported in this paper has been partly supported by the Grant-in-Aid for Scientific Research on Priority Areas "Theory of Chemical Reaction — Computational Approach" from the Ministry of Education, Science, and Culture of Japan.

[1] M. J. Seaton, Proc. Phys. Soc. London **77**, 174 (1961).
[2] M. Gailitis and R. Damburg, Proc. Phys. Soc. London **82**, 192 (1963).
[3] A. J. Taylor and P. G. Burke, Proc. Phys. Soc. London **92**, 336 (1967).
[4] J. Macek, Proc. Phys. Soc. London **92**, 365 (1967).
[5] J. W. McGowan, J. F. Williams, and F. K. Carley, Phys. Rev. **180**, 132 (1969).
[6] J. F. Williams and B. A. Willis, J. Phys. B **7**, L61 (1974).
[7] H. C. Bryant, B. D. Dieterie, J. Donahue, H. Sharifian, H. Tootoonchi, D. M. Wolfe, P. A. M. Gram, and M. A. Yates-Williams, Phys. Rev. Lett. **38**, 228 (1977).
[8] M. E. Hamm, R. W. Hamm, J. Donahue, P. A. M. Gram, J. C. Pratt, M. A. Yates, D. R. Bolton, D. A. Clarke, H. C. Bryant, C. A. Frost, and W. W. Smith, Phys. Rev. Lett. **43**, 1715 (1979).
[9] P. G. Harris, H. C. Bryant, A. H. Mohagheghi, R. A. Reeder, H. Sharifian, C. Y. Tang, H. Tootoonchi, J. B. Donahue, C. R. Quick, D. C. Rislove, W. W. Smith, and J. E. Stewart, Phys. Rev. Lett. **65**, 309 (1990).
[10] M. Halka, H. C. Bryant, E. P. MacKerrow, W. Miller, A. H. Mohagheghi, C. Y. Tang, S. Cohen, J. B. Donahue, C. Johnstone, B. Marchini, A. Hsu, C. R. Quick, J. Tiee, and K. Rozsa, Phys. Rev. A **44**, 6127 (1991); M. Halka (private communication).
[11] M. Halka, H. C. Bryant, C. Johnstone, B. Marchini, W. Miller, A. H. Mohagheghi, C. Y. Tang, K. B. Butterfield, D. A. Clark, S. Cohen, J. B. Donahue, P. A. M. Gram, R. W. Hamm, A. Hsu, D. W. MacArthur, E. P. MacKerrow, C. R. Quick, J. Tiee, and K. Rózsa, Phys. Rev. A **46**, 6942 (1992).
[12] H. A. Hyman, V. L. Jacobs, and P. G. Burke, J. Phys. B **5**, 2282 (1972).
[13] J. T. Broad and W. P. Reinhardt, Phys. Rev. A **14**, 2159 (1976).
[14] C. R. Liu, N. Y. Du, and A. F. Starace, Phys. Rev. A **43**, 5891 (1991).
[15] H. R. Sadeghpour, C. H. Greene, and M. Cavagnero, Phys. Rev. A **45**, 1587 (1992).
[16] J.-Z. Tang, S. Watanabe, and M. Matsuzawa, Phys. Rev. A **46**, 2437 (1992).
[17] J. Macek, J. Phys. B **1**, 831 (1964).
[18] J.-Z. Tang, S. Watanabe, and M. Matsuzawa, Phys. Rev. A **46**, 3758 (1992).
[19] J.-Z. Tang, S. Watanabe, M. Matsuzawa, and C. D. Lin, Phys. Rev. Lett. **69**, 1633 (1992).
[20] J.-Z. Tang, S. Watanabe, and M. Matsuzawa, Phys. Rev. A **48**, 841 (1993).
[21] L. D. Landau and E. M. Lifshitz, *Quantum Mechanics*, 3rd ed. (Pergamon Press, Oxford, 1977).
[22] C. H. Greene, U. Fano, and G. Strinati, Phys. Rev. A **19**, 1485 (1979).
[23] C. L. Pekeris, Phys. Rev. **126**, 1470 (1962).
[24] P. M. Dehmer and W. A. Chupka, Bull. Am. Phys. Soc. **20**, 729 (1975).
[25] D. R. Herrick and O. Sinanoglu, Phys. Rev. A **11**, 97(1975); D. R. Herrick, *ibid.* **12**, 413 (1975).
[26] C. D. Lin, Phys. Rev. A **29**, 1019 (1984); Adv. At. Mol. Phys. **22**, 77 (1986).
[27] The quantum numbers n and n' are often denoted by N and n as in our previous papers [16,19,20].
[28] A. Pathak, A. E. Kingston, and K. A. Berrington, J. Phys. B **21**, 2939 (1988).
[29] J. F. Williams, J. Phys. B **21**, 2107 (1988).
[30] H. R. Sadeghpour and C. H. Greene, Phys. Rev. Lett. **65**, 313 (1990).
[31] Y. K. Ho, Phys. Rev. A **45**, 148 (1992).
[32] J. J. Wendoloski and W. P. Reinhardt, Phys. Rev. A **17**, 195 (1978).
[33] J. Callaway, Phys. Lett. **68**A, 315 (1978); Phys. Rev. A **26**, 199 (1982); **37**, 3692 (1988).
[34] M. Cortés and F. Martín, Phys. Rev. A **48**, 1227 (1993).